

TUSK PALEOHISTOLOGY AS A TOOL IN THE DISCRIMINATION OF FOSSIL TUSKS FROM GREECE

Konstantina AGIADI & George THEODOROU

AGIADI, K. & THEODOROU, G. 2005. Tusk Paleohistology as a tool in the discrimination of fossil tusks from Greece. In ALCOVER, J.A. & BOVER, P. (eds.): *Proceedings of the International Symposium "Insular Vertebrate Evolution: the Palaeontological Approach"*. *Monografies de la Societat d'Història Natural de les Balears*, 12: 1-8.

Resum

En aquest estudi intentam discriminar entre les defenses de *Mammuthus meridionalis*, *Elephas antiquus* i les dels elefants nans de l'illa de Tilos, en base a les característiques histològiques de la dentina. El tret mesoscòpic examinat és el Patró d'Schreger, en relació a l'angle, la longitud d'ona i l'aparença qualitativa, i els trets microscòpics són la mida dels túbuls de dentina i la seva densitat. Les mostres de defenses de mamut es diferencien clarament de les d'elefants. A més, trobam una petita variança en l'aparença qualitativa del Patró d'Schreger entre les mostres d'*Elephas antiquus* i les defenses dels elefants nans. Finalment, la mida dels túbuls de dentina de les defenses dels elefants endèmics és, clarament, la major.

Paraules clau: defenses, Paleohistologia, dentina, elefants nans, *Elephas antiquus*, *Mammuthus meridionalis*.

Summary

In the current study, we have attempted to distinguish between the tusks of *Mammuthus meridionalis*, *Elephas antiquus* and the dwarf elephants from the island of Tilos, based on the tusk dentine's histological characteristics. The mesoscopic feature examined is the Schreger Pattern, in respect to its angle, wavelength and qualitative appearance, and the microscopic features are the dentinal tubule's size and density. The mammoth samples strongly discriminate against the elephant tusks. In addition, we were able to find a small variance in the Schreger Pattern's qualitative appearance, between the samples of *Elephas antiquus* and the tusks of the dwarfs. Finally, the size of the dentinal tubules is clearly greatest in the tusks of the endemic elephants.

Key words: tusks, Palaeohistology, dentine, dwarf elephants, *Elephas antiquus*, *Mammuthus meridionalis*.

INTRODUCTION

The aim of this study is to compare the dwarf elephant tusks, found on the island of Tilos, to those of *Elephas antiquus* and *Mammuthus meridionalis*, in respect to the dentine's histological characteristics. In the past, Proboscidean tusk dentine has been used to distinguish tusks and tusk fragments of different taxa (Espinoza & Mann, 1993; Fisher *et al.*, 1998; Palombo & Villa, 2001; Palombo, 2003). For the most part though, these examinations included only the Schreger angle. On previous papers (Agiadi, 2001; Theodorou & Agiadi, 2001; Agiadi, 2003), we have examined other histological features, namely the dentinal tubule density and diameter. At the same time, Trapani & Fisher (2003) used the Schreger Pattern's angle, wavelength, and qualitative appearance, to distinguish between tusks of mammoths (*M. primigenius* and *M. columbi* undifferentiated), mastodons (*Mammuth americanum*) and extant elephants (*Elephas maximus* and *Loxodonta africana*). In the current study, we examine for the first time all the above features in conjunction, in order to discriminate between tusks of

Elephas antiquus and *Mammuthus meridionalis*, the two Proboscidean taxa, which dominated the Greek Peninsula during the Quaternary. Furthermore, we compare the obtained results to the corresponding ones for the dwarf elephant tusks from the Tilos Island. Specifically, the characteristics examined herein (Fig.1) are: the Schreger angle (*sa*), the Schreger Pattern's phenomenon wavelength (*w*), the Schreger Pattern's qualitative appearance (*q*), the dentinal tubule density (*dtd*) and the dentinal tubule diameter (*tdi*).

The material used for the present study (Table 1) consists of: 1) two tusks from the Lower Pleistocene locality of Vlachioti (Lakonia, Peloponnisos, Greece), which have been attributed to *Mammuthus (Archidiskodon) meridionalis*, by identification of other skeletal and dental material (Symeonidis & Theodorou, 1986), 2) one tusk found near the village Nissoi (Ileia, Peloponnisos, Greece) by Associate Prof. Theodorou during a field trip to the area on July 1994. According to Assoc. Prof. Theodorou, this specimen exhibits the typical features of *Elephas antiquus* and is consequently attributed to this species (data under publication), 3) five tusks from the area of Megalopolis (Arcadia, Pelopo-

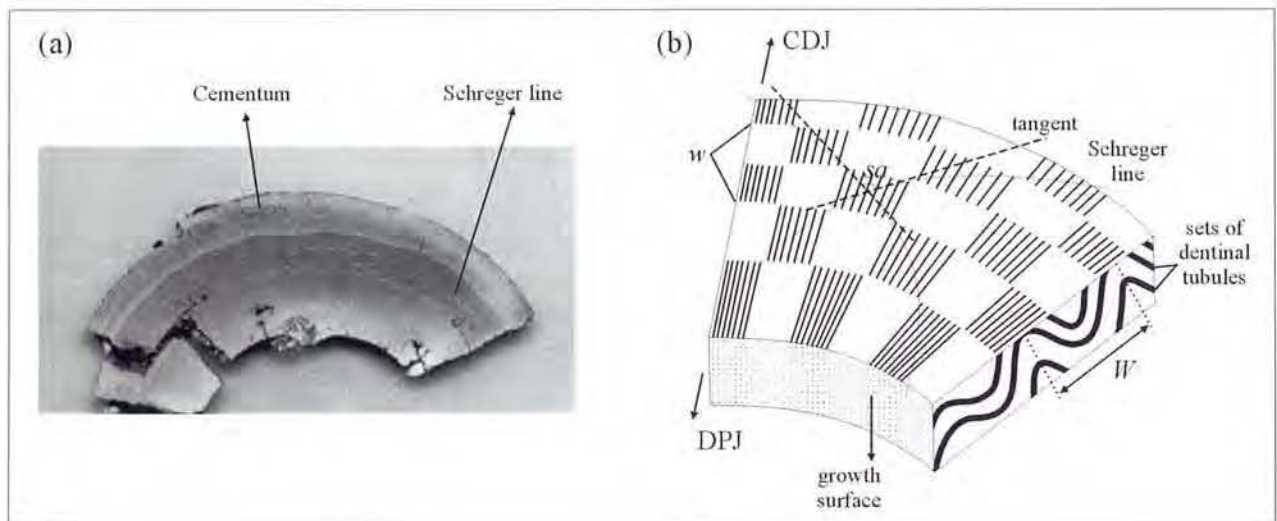


Fig. 1.
 (a) Polished transverse section of a tusk belonging to a dwarf elephant from Tilos (T.00/144). On the outermost part we can see the thin layer of cementum, covering the dentine. The first layer of dentine, adjacent to the cementum-dentine junction (CDJ), is called mantle dentine. In the extant elephant species, this layer has a thickness of 40–80 μm , and is characterized by irregularly spaced, extensively branched dentinal tubules, which are strongly curved toward the tip of the tusk (Raubenheimer et al., 1998). Underneath the mantle dentine there is the main part of the tusk's dentine, which exhibits the Schreger Pattern.
 (b) Schematic block diagram of the tusk's dentine, presenting the Schreger Pattern features. The growth surface coincides with the circumferential view of the dentine. The Schreger Pattern is visible on the transversal view, whilst on the radial view we can see part of the sinusoidal organization of the sets of dentinal tubules. As we can observe on this diagram, the true dentinal tubule wavelength (W) remains constant, while the angle between the sinusoidal direction of the tubules and the transversal view changes as we move from the dentine-pulp junction (DPJ) towards the CDJ. As a result, the phenomenon Schreger Pattern wavelength (w) increases towards the DPJ. The phase difference between the sinusoidal movement of adjacent bundles of odontoblasts, when it is projected on the transversal plane of the tusk, results in the intersecting Schreger lines. On the transverse section, we can measure the Schreger angle (sa), by drawing the tangents to the Schreger lines.

Fig. 1.
 (a) Secció transversal polida d'una defensa pertanyent a un elefant nan de Tilos (T.00/144). A la part més exterior podem veure una capa prima de ciment, la qual cobreix la dentina. La primera capa de dentina, adjacent a la unió ciment-dentina (CDJ) s'anomena dentina mantell. A les espècies d'elefants vivents aquesta capa té un gruix de 40–80 μm , i es caracteritza per túbuls de dentina extensament ramificats, espaiats irregularment, que estan fortament corbats cap a l'extrem de la defensa (Raubenheimer et al., 1998). Per sota de la dentina mantell es troba la part principal de la dentina de la defensa, la qual exhibeix el Patró d'Schreger.
 (b) Diagrama de blocs esquemàtic de la dentina de les defenses, presentant els trets del Patró d'Schreger. La superfície de creixement coincideix amb la norma circumferencial de la dentina. El Patró d'Schreger és visible en norma lateral, mentre que en norma radial podem veure part de l'organització sinusoidal dels conjunts de túbuls de dentina. Com podem observar, a aquest diagrama, la veritable longitud d'ona dels túbuls de dentina (W) roman constant, mentre que l'angle entre la direcció sinusoidal dels túbuls i la norma transversal canvia a mesura que ens movem des de la unió polpa-dentina (DPJ) cap a la CDJ. Com a resultat, el fenomen de la longitud d'ona del Patró d'Schreger (w) s'incrementa cap al final del DPJ. La diferència de fase entre el moviment sinusoidal dels bonyos adjacents d'odontoblastes resulta en la intersecció de línies d'Schreger. A la secció transversa podem mesurar l'angle d'Schreger (sa) dibuixant les tangents a les línies d'Schreger.

nnisos, Greece) identified by Melentis (1961) as belonging to *Elephas (Palaeoloxodon) antiquus*, 4) two tusk pieces also from Megalopolis (Melentis, 1961), which belong to *Mammuthus meridionalis*, and 5) fourteen tusks and tusk pieces found in the Charkadio Cave (Tilos, Dodekanese islands, Greece). It has been noted by previous studies (Theodorou, 1983), that no proof of any interaction between the dwarf elephants from Tilos islands and the dwarfs from Malta has been provided to date. Consequently, the two endemic evolutionary phenomena have progress separately. However the fossil elephant material found on the island of Tilos is still provisionally attributed to *Palaeoloxodon antiquus falconeri* (Theodorou, 1983).

Concerning methodology, the structure of the tusks' dentine was observed by combination of mesoscopic and microscopic investigation. The features were observed in detail using an optical petrographic and a scanning electron microscope (S.E.M.), under various magnifications. For this purpose, transverse sections were cut and thin sections were prepared whenever necessary. Our observations mainly concerned the perpen-

	<i>Mammuthus meridionalis</i>	<i>Elephas antiquus</i>	Dwarf elephants
sa	83–128 degrees	131–158 degrees	108–158 degrees
w	0.55–0.95 mm	0.56–0.92 mm	0.47–0.87 mm
q	Uniform throughout dentine's thickness, "X", occasionally "C"	"V" and some "X"	"V/C" on the outer zone, "X" on the inner zone
dtd	25500–43000 dt/mm ²	18300–40365 dt/mm ²	11524–45500 dt/mm ²
tdi	1.0–2.0 μm	0.5–1.0 μm	2.1–2.9 μm

Table 2. Identifying and discriminating characteristics of the tusk dentine of *Mammuthus meridionalis*, *Elephas antiquus*, and the dwarf elephants from the island of Tilos. The Schreger Pattern's features (angle, wavelength and qualitative appearance) are observed macroscopically, as well as under the optical microscope, while the dentinal tubules can only be seen under high magnification, with the use of a scanning electron microscope.

Taula 2. Trets diferencials característics de la dentina de les defenses de *Mammuthus meridionalis*, *Elephas antiquus*, i dels elefants nans de l'illa de Tilos. Les característiques dels Patrons d'Schreger (angle, longitud d'ona i semblança qualitativa) s'observen macroscòpicament, igual que amb un microscopi òptic, mentre que els túbuls de dentina només es poden veure a grans augments, amb l'ús del microscopi electrònic d'escandallatge.

dicular plane to the tusks' axes, since this is the direction where the Schreger Pattern appears. Only stub samples examined under the S.E.M. were orientated parallel to the tusks' long axes and outer surfaces (circumferential plane), so that we could measure the dentinal tubule's density and diameter. Occasionally, we also examined stubs on the radial direction, in order to see the longitudinal sections of the dentinal tubules.

In order to evaluate the Schreger Pattern's characteristics, on our samples, pieces of the tusks were encased in polyester resin. The blocks were cut perpendicularly to the tusks' axes and were then polished thoroughly with emery dust of two sizes. Afterwards the polished surfaces were scanned and the *sa* was measured at high magnification, using image processing software. In particular, the program CorelDraw vs.10 was used for this purpose. The scanned pictures were processed to enhance the Schreger lines. Then, under magnification, the tangents were drawn on each side of the angle. The *sa* was measured on the printouts. For the purpose of measuring the *w* and to characterize the *q*, thin sections were cut, using the same encased fragments. We must note, at this point, that the classification of the Schreger Pattern's qualitative appearance follows here the categories proposed by Trapani & Fisher (2003). In particular, these authors separated three main cate-

gories, "V", "C", and "X". When we observe a transverse section of the tusk, i.e. perpendicular to the growth surfaces, the "V" pattern occurs when there are continuous lines, oblique to the incremental features, with one direction (dextral or sinistral), being locally dominant. The "C" pattern consists of rectangular light and dark areas resembling a checkerboard. The diagonally neighbouring dark or light areas may share only a corner, or may be more broadly confluent. Finally, the "X" pattern is described as having criss-crossing continuous lines, oblique to the incremental features and occurring in both dextral and sinistral direction [Trapani & Fisher, 2003].

ABBREVIATIONS

<i>sa</i>	Schreger angles
<i>w</i>	Schreger Pattern's phenomenon wavelength
<i>q</i>	Schreger Pattern's qualitative appearance
<i>dt</i>	dentinal tubule density
<i>tdi</i>	dentinal tubule diameter
S.E.M.	Scanning Electron Microscope
S.P.	Schreger Pattern
CDJ	cementum-dentin

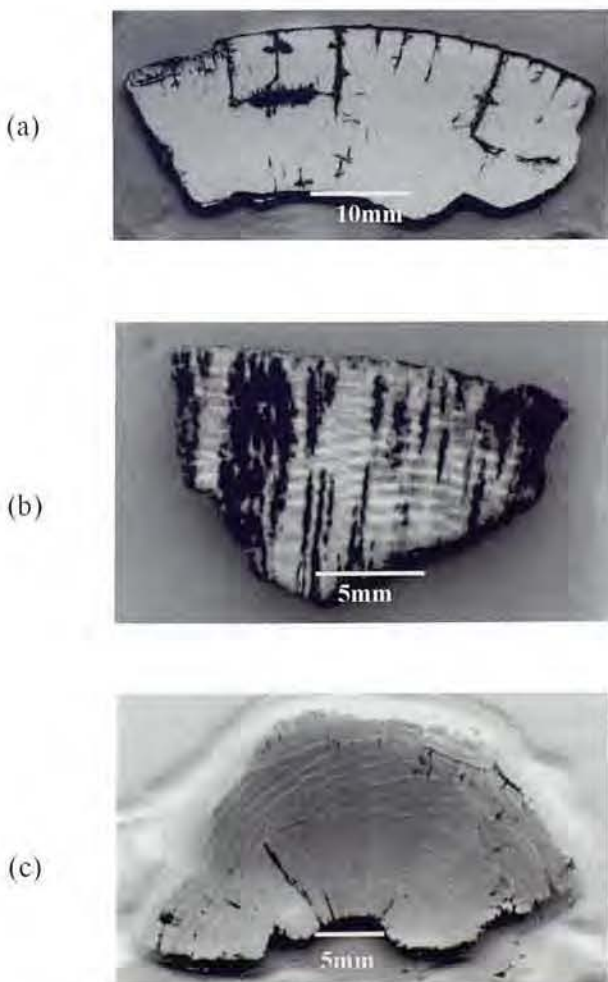


Fig. 2. According to Trapani & Fisher (2003), there are three categories of qualitative appearance that can be used to classify the Schreger Pattern. The "V" pattern consists of "continuous lines, oblique to the incremental lines, with one direction locally dominating"; "Rectangular light and dark areas resembling a checkerboard, with the diagonally neighboring dark or light areas sharing only corners", result in the "C" type of Schreger Pattern. If however the Pattern is made of "criss-crossing continuous lines, oblique to the growth increments, occurring in both dextral and sinistral directions", then we place this to the "X" category. We can also distinguish the intermediate categories "X/C", "V/C", and "X/V".

- (a) Transverse section on a tusk piece of *Mammuthus meridionalis* from Vlachioti (Lakonia). We can see that the dominant feature is "X/C".
- (b) Transverse section on a tusk piece of *Elephas antiquus* from Nissoi (Ileia), where we can observe mostly "V", and rarely "X" patterns.
- (c) Transverse section on a tusk piece from a dwarf elephant (Tilos, Dodekanese). On the outer zone of the Pattern, we can clearly observe the "C" type, which changes to "V" towards the pulp cavity. The "X" type can be seen only on the inner zone.

Fig. 2. D'acord amb Trapani & Fisher (2003) hi ha tres categories de semblança qualitativa que poden ser emprades per a classificar el Patró d'Schreger. El patró en "V" consisteix en "línies contínues, obliqües a les línies d'increment, amb una direcció localment dominant". El tipus "C" del Patró d'Schreger consisteix en "àrees rectangulars clares i fosques que s'assemblen a una taula d'escacs, amb les àrees clares i fosques properes diagonalment compartint només els cantons". No obstant, si el Patró està fet per "línies contínues entrecreuadaes, obliqües als increments de creïement, que es donen tant en direcció dreta com esquerra" ens trobam a la categoria "X". També podem distingir les categories intermèdies "X/C", "V/C", i "X/V".

- (a) Secció transversa d'una peça de defensa de *Mammuthus meridionalis* de Vlachioti (Lakonia). Podem veure que el tret dominant és "X/C".
- (b) Secció transversa d'una peça de defensa d'*Elephas antiquus* de Nissoi (Ileia), on podem observar principalment patrons "V" i rarament "X".
- (c) Secció transversa d'una peça de defensa d'un elefant nan (Tilos, Dodecanès). A la zona externa del Patró podem observar clarament el tipus "C", amb canvis cap a "V" cap a la cavitat polpar. El tipus "X" només es pot veure a la zona interna.

TUSK PALEOHISTOLOGY

Proboscidean tusks are enlarged incisors formed by orthodontine, which is covered on the outer surface by a thin layer of cellular cementum. Enamel, in the species examined here, is found only as a very thin layer, covering the tip of the tusks. Due to the special functions and the consequent enlargement of tusks, the dentine has formed certain features, unique to Proboscidean tusks, which combine to produce the Schreger Pattern (S.P.). This Pattern was first observed, by Bernard Schreger (1800), on sections perpendicular to the tusk's axis. It consists of two sets of light and dark lines, radiating from the outer dentine surface, towards the axis of the tusk, in a spiral fashion. One set of Schreger lines radiates clockwise and the other counter-clockwise, thus intersecting to form the Schreger angles.

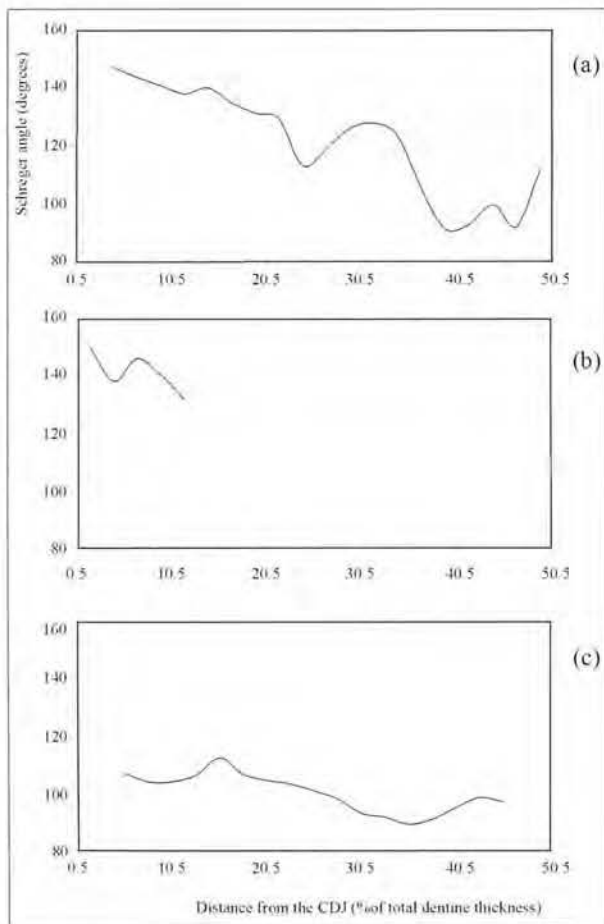


Fig. 3. The Schreger angle in relation to the distance from the cementum-dentine junction (CDJ). The distance is expressed as a percentage of the total dentine thickness at the position of each measurement.

- (a) Diagram for the dwarf elephant tusks.
- (b) Diagram for *Elephas antiquus* from Megalopolis.
- (c) Diagram for *Mammuthus meridionalis* from Vlachioti.

Fig. 3. L'angle d'Schreger en relació a la distància des de la unió ciment-dentina (CDJ). La distància s'expressa com a percentatge del gruix total de dentina a la posició de cada mesura presa.

- (a) Diagrama per a les defenses d'elefants nans.
- (b) Diagrama per a *Elephas antiquus* de Megalopolis.
- (c) Diagrama per a *Mammuthus meridionalis* de Vlachioti.

The Schreger Pattern (Fig. 1a) is the macroscopic manifestation of the microscopic architecture of tusk dentine. During odontogenesis, as the odontoblasts move towards the proximocentral part of the tusk's pulp cavity, they leave behind them the dentinal tubules, which are the traces of the odontoblasts' sinusoidal movement (Raubenheimer *et al.*, 1998). As a result, when observing a transverse section of the tusk, we can essentially observe the undulation of the dentinal tubules, projected as the dark and light lines of the Schreger Pattern (Figs. 1 & 2). Dark lines correspond to the concave part of the undulation, while the light lines represent the convex part. The fact that, on a transverse section, we do not observe alternating light and dark concentric rings, but rather the dextral and sinistral Schreger lines, leads to the conclusion that the periodic movement of the odontoblasts, towards the proximocentral part of the pulp cavity, does not occur simultaneously for the entire band of odontoblastic cells. On the contrary, the cells are organized in bundles that move simultaneously, producing sets of dentinal tubules, which are in phase with each other, but have a phase difference of π , in relation to the neighbouring sets.

In respect to all the above, the parameters characterizing the Schreger Pattern are the size and density of the dentinal tubules, the wavelength of their undulation, and the size of the dentinal tubule sets. These parameters are defined by the shape of the original pulp cavity, the size and density of the odontoblasts and the rate of dentine deposition, which in turn produce the final shape and size of the tusk. On the circumferential view of the tusk, we can directly measure the size and density of the dentinal tubules. Also, on a transverse section of the tusk, we measure the Schreger Pattern phenomenon wavelength, as the distance between two adjacent dark or light lines. As for the size of the dentinal tubule sets, this is expressed instead by the Schreger angles, which we also measure on transverse sections.

OBSERVATIONS

Mammuthus meridionalis

The Schreger Pattern on *M. meridionalis*, as observed on the transversal plane, appears continuously throughout the thickness of the tusk's dentine. The *sa* decreases from the outermost surface of the dentine towards the pulp cavity. Measurements of the *sa*, on the outer approximate 45% of the dentine's thickness, give values between 83° - 128° , with the maximum value appearing at 15%. Fig. 3c shows the relationship between the *sa* values and the distance from the outer dentine surface. There are four areas of deviation, from the general decrease of the *sa*, namely at: 13.6-19.1% (maximum value of *sa* at 16.4%), 21.8-23.6% (max at 22.7%), 26.4-28.2% (max at 27.5%), and 40%-48.2% (max at 43.6%). Regarding the *w*, measurements were made at the same area as the *sa* and produced values between 0.55-0.95 mm. Qualitatively the Schreger Pattern exhibits mostly "X" patterns and occasionally "C" patterns, as those were described by Trapani

& Fisher (2003) (Fig. 2a). We are not able to distinguish any "V" patterns, although our examination does not include the inner part of the tusk's thickness, where the above authors mention the appearance of the "V" pattern on the tusks of *M. primigenius* and *M. columbi*.

On the microscopic level, we observe the organization of the dentinal tubules (Fig. 4a & b), and measure their *tdi* and *dt*, near the cementum-dentine junction (CDJ), but below the mantle dentine. Due to the sinusoidal movement of the odontoblasts, the dentinal tubule sections, on a circumferential view of the tusk's dentine, are ellipses with their large diameters parallel to the direction of the tusk's axis. Thus the large diameter of an elliptical section is a phenomenon diameter of the tubule. Additionally, the lateral component of the odontoblasts' movement is relatively small, and it varies amongst adjacent tubules in a sinuous fashion. Consequently, calculating the mean tubule small diameter, for an area of about $11 \cdot 10^{-3} \text{ mm}^2$, should eliminate the fluctuation due to the lateral movement. As a result we accept this mean value as the true dentinal tubule diameter (*tdi*). For the samples of *Mammuthus meridionalis* the measurement of the dentinal tubule small diameter produces values between 1.0-2.0 μm . On the same circumferential microscopic views, we also measured the *dt*, which ranges from 25500 to 43000 dt/mm². Both the *tdi* and *dt* was measured on a total of 20 samples.

Elephas antiquus

The tusks of *E. antiquus* from both localities exhibited the same microstructural features. The *sa* decreases from the outer part of the dentine towards the pulp cavity. Measurements of the *sa* were taken only within the outer 15% of the dentine's thickness (Fig. 3b), because our tusk samples did not allow for the separation of a larger piece. The *sa* ranges between 131° - 158°, reaching a maximum at 5.8% of the dentine's thickness, which also constitutes an irregularity in the general decrease of the *sa* toward the central tusk axis. It is important to note, at this point, that the *sa* was measured in our samples only in relation to the distance from the cementum-dentine junction, because we have previously established that there is no particular pattern of a *sa* variation along the proximodistal direction, i.e. the Schreger Pattern does not change with the age of the tusk, but rather depends on the shape of the pulp cavity (Theodorou & Agiadi, 2001). This allows us to use tusk fragments even though their position along the tusk was not always known. Qualitatively, the Schreger Pattern exhibits mostly "V" and some "X" patterns. In addition, the *w* ranges between 0.56-0.92 mm, increasing towards the pulp cavity.

Regarding the dentinal tubules' size and distribution (Figs. 4c & 5a), we measure the *dt* on stubs taken from both the areas near the cementum-dentine and the pulp-dentine junction. There does not appear to be any significant differentiation of this characteristic, among the two areas. In particular, the *dt* measures between 18300-40365 dt/mm². Furthermore we measure the mean dentinal tubule small diameter, which is the true dentinal tubule diameter (*tdi*), at the same areas, to range between 0.5-1.0 μm . The total number of samples examined for *tdi* and *dt* was 18.

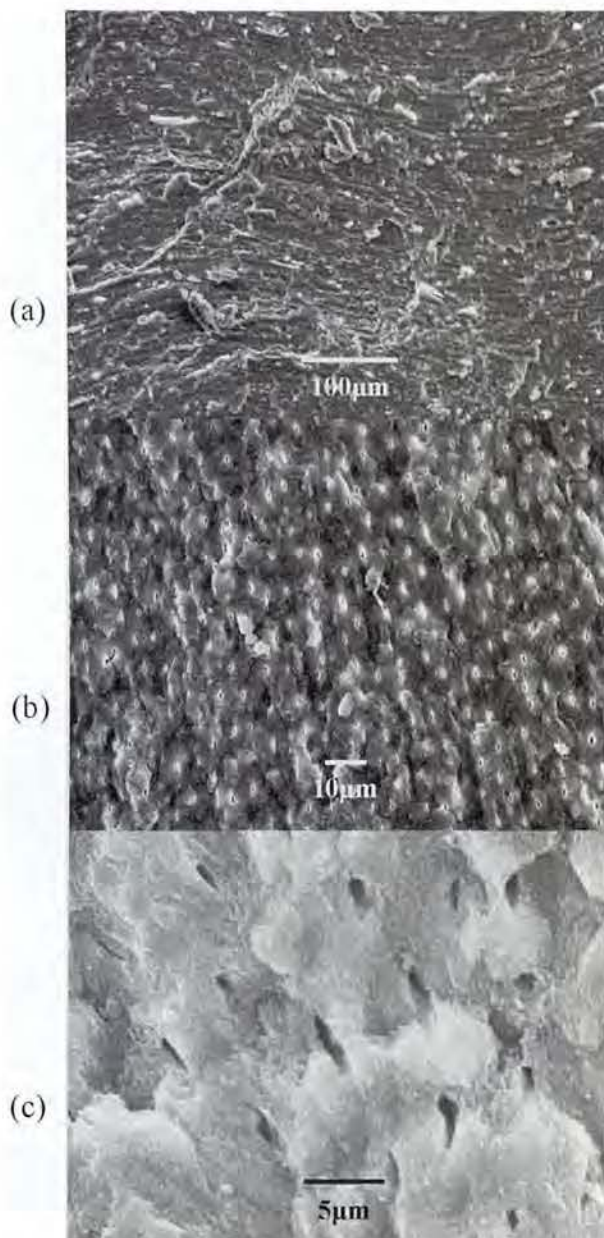


Fig. 4. S.E.M. images of tusk dentine, showing the distribution of the dentinal tubules.

- Tusk specimen of *Mammuthus meridionalis* from Vlachioti (Lakonia), where a stub has been taken at a distance of about 7.0 mm from the CDJ. We can see the transverse sections of the dentinal tubules.
- On the same specimen, we have a radial view of the dentine, where we can see the longitudinal sections of the undulating dentinal tubules.
- Tusk specimen of *Elephas antiquus* (1960/183), stub taken from the outer dentine layers, at about 9.5 mm from the CDJ. We observe oblique sections of the dentinal tubules, at a view almost parallel to a growth surface.

Fig. 4. Imatges SEM de la dentina de les defenses, mostrant la distribució dels túbuls de dentina.

- Mostra de defensa de *Mammuthus meridionalis* de Vlachioti (Lakonia), on s'ha agafat una peça a una distància de 7,0 mm del CDJ. Podem veure les seccions transverses dels túbuls de dentina.
- Al mateix exemplar, tenim una vista radial de la dentina, on es poden veure les seccions longitudinals dels túbuls de dentina ondulants.
- Mostra de defensa d'*Elephas antiquus* (1960/183), peça agafat a les capes de dentina exterior, a devers 9,5 mm del CDJ. Observam seccions obliques dels túbuls de dentina, en norma quasi paral·lela a la superfície de creixement.

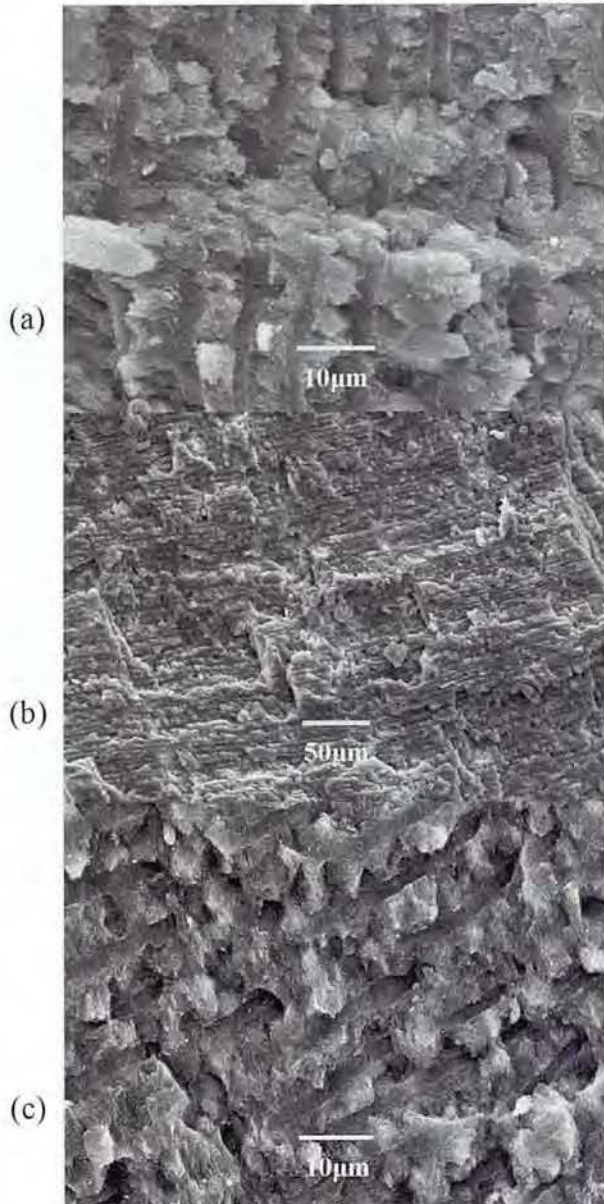


Fig. 5. S.E.M. images of tusk dentine, showing the distribution of the dentinal tubules.

- (a) Tusk specimen of *Elephas antiquus* from Nissoi (Ileia), where we can see nearly longitudinal sections of the dentinal tubules.
- (b) Radial view of a dwarf tusk (unnumbered sample), where we can see the longitudinal sections of the undulating dentinal tubules. The width of the undulation is greater than that on the specimens of *M. meridionalis*.
- (c) Oblique sections of the dentinal tubules, at an almost radial view of the same sample.

Fig. 5. Imatges SEM de la dentina de les defenses, mostrant la distribució dels túbuls de dentina.

- (a) Mostra de defensa d'*Elephas antiquus* de Nissoi (Ileia), on podem veure seccions quasi longitudinals dels túbuls de dentina.
- (b) Vista radial d'una defensa d'elefant nan (mostra no numerada), on podem veure les seccions longitudinals dels túbuls de dentina ondulants. L'amplada de l'ondulació és major que als espècimens de *M. meridionalis*.
- (c) Seccions obliqües dels túbuls de dentina, en una vista quasi radial de la mateixa mostra.

On the transverse sections of the Tilos elephant tusks, we can clearly distinguish two zones of dentine, with obvious differences in the Schreger Pattern's qualitative and quantitative characteristics. The qualitative appearance exhibits a combination of "V" and "C" patterns on the outer zone, with "C" patterns dominating as we move towards the CDJ. The "X" type of Schreger Pattern is confined to the inner zone, where we sometimes also observe the "V" type. We concentrate on the Schreger angle variance regarding the outer zone, so that our results would be comparable to our measurements on the samples of the other species. To this end, we examined approximately the outermost 50% of the dentine's thickness. Our *sa* values for this show a range from 108° to 158° . By plotting the *sa* against the distance from the CDJ, on the specimen T.00/144, we confirm its decrease toward the tusk's axis. However there is an anomaly, between 26-36% of the dentine's thickness, with a maximum being achieved at about 31% (Fig. 3a). Finally, on the same areas, we also measured the *w*, which varies between 0.47-0.87 mm, increasing towards the pulp cavity.

Microscopically, the *dtd* on our samples has a range from 11524 to 45500 dt/mm², and the *tdi* varies between 2.1-2.9 µm (Fig. 5b & c). We examined 13 stub samples from the tusks, each time noting their position on the specimen. There is no differentiation of the size and density values, along the periphery of the tusks, or across the radial, although the greatest density values (*dtd* > 35000 dt/mm²) can indeed be measured on the outermost part of the dentine. However this can be explained by the existence of the mantle dentine, which is characterized by an extreme branching of the tubules.

DISCUSSION

In the present study, we have reached valuable results, which further our understanding of the Schreger Pattern. The Schreger angle is related to the phenomenon wavelength and the width of the dentinal tubule sets, in a given position in the tusk (Fig. 1b). The *sa* increases towards the CDJ and so does the sets' width, but the wavelength decreases. Although we have not examined the relationship between the Pattern's wavelength and the distance from the CDJ, we expect it to be similar to that observed between the angle and the CDJ distance. Such a pattern would be able to differentiate between taxa in the similar manner. However, simply comparing the range of the wavelength, in a given part of the tusks' thickness, does not provide any discrimination. Regarding the Schreger Pattern's qualitative appearance, this depends on how abrupt the boundaries of the tubule sets are. When they are very abrupt, we observe the "C" pattern. When the boundaries on direction are abrupt, and on the other smooth, they produce the "V" pattern. And finally, smooth boundaries, i.e. progressive transmission of the proximocentral movement of the odontoblasts, produce the "X" type of pattern.

Locality	Taxon	L (cm)	d1 (cm)	d2 (cm)	Specimen
Vlachioti	<i>M.meridionalis</i>	100.0	12.00*	9.50*	unnumbered (sin.)
Vlachioti	<i>M.meridionalis</i>	44.5	11.80*	10.30*	unnumbered (dext.)
Nissoi	<i>E. antiquus</i>	265.0	18.64	17.46	NS. 1994/1
Megalopolis	<i>E. antiquus</i>	145.5	15.30	14.5	1960/94 (dext., M.)
Megalopolis	<i>E. antiquus</i>	186.0	8.60	8.00	1960/96 (sin., F)
Megalopolis	<i>E. antiquus</i>	77.5	6.70	6.60	1960/183 (sin. E)
Megalopolis	<i>E. antiquus</i>	51.0	6.20	6.00	1960/187 (dext., M.)
Megalopolis	<i>E. antiquus</i>	289.5	16.40	15.00	1960/188 (sin.M.)
Megalopolis	<i>M. meridionalis</i>	87.0	9.30	7.50	1960/182 (F)
Megalopolis	<i>M. meridionalis</i>	145.0	11.90	10.10	1960/95 (dext., F)
Charkadio cave	dwarf elephants	47.0	9.50	7.50	T.00/53
Charkadio cave	dwarf elephants	20.55	4.05	3.65	T.00/144
Charkadio cave	dwarf elephants	42.0	3.84	3.74	T.70/1999 (sin., E)
Charkadio cave	dwarf elephants	28.5	2.85	2.75	T.1/98 (sin., d)
Charkadio cave	dwarf elephants	25.5	2.40	2.17	T.00/41 (d)
Charkadio cave	dwarf elephants	40.5	3.51	3.20	T.85/91 (sin., F)
Charkadio cave	dwarf elephants	39.0	4.15	3.61	T.89/91
Charkadio cave	dwarf elephants	49.0	4.14	3.78	T.10481 (sin., F)
Charkadio cave	dwarf elephants	44.5	3.98	3.47	T.143b/82 (M.)
Charkadio cave	dwarf elephants	42.5	4.22	3.80	T.143a/82
Charkadio cave	dwarf elephants	50.5	4.38	4.01	T.293/98 (dext., F)
Charkadio cave	dwarf elephants	-	-	-	unnumbered
Charkadio cave	dwarf elephants	-	-	-	T.354/99 (d)
Charkadio cave	dwarf elephants	68.0	7.14	6.69	T.88/91 (dext., F)

Table 1. Tusk material examined in this study, including macroscopic measurements. L: tusk or tusk piece's length following the proximo-distal direction in a straight line, d1: maximum diameter at approximately the middle of the tusk's length, d2: minimum diameter at the same position. The measurements followed by * have been taken at the proximal end of the tusk. All of the specimens are deposited in the Museum of Palaeontology and Geology of the University of Athens.

Taula 1. Material de defenses examinat a aquest estudi, incloent les mesures macroscòpiques. L: llargària de la defensa o part de la defensa disponible seguint la direcció proximo-distal en línia recta. d1: diàmetre màxim agafat aproximadament a la meitat de la llargària de la defensa, d2: diàmetre mínim a la mateixa situació. Les mesures seguides per un asterisc han estat preses a la part proximal de la defensa. Tots els espècimens estan dipositats al Museu de Paleontologia i Geologia de la Universitat d'Atenes.

Very important also are the microstructural observations, which once more present the uniqueness of the tusk dentine tissue. Concerning the microstructural features of dentine, the dentinal tubule density does not present any discriminating power, in the samples examined herein. Besides, the tissue is the same in all three taxa, and would be expected to have the same needs in intratubular material (odontoblastic material, neural fibers, etc.). In addition, there appears to be no variance in density amongst different areas of the dentine's thickness, a fact also expected for the same reasons. The dentinal tubule's branching process, in this case, compensates for the increased periphery of the tusk, as we move toward the outer part. However the dentinal tubule size differs between our samples. In particular, the tusks of the dwarf elephants from Tilos island have much larger tubules, than the samples of *Elephas antiquus* and *Mammuthus meridionalis*. The reasons for this differentiation are not yet clear to us. Although the fossilization

processes could have affected this feature, a low degree of calcification, in the first place, may account for the larger tubule diameter found in the tusks of the dwarfs. In such a case, we should think that the smaller and lighter tusks of the dwarf elephants have less need for solidity and resistance to stress than do the ones of larger animals.

Comparing the results for the tusks from the three taxa (Table 2), distinction of mammoths from elephants is clear, by means of the Schreger angle and qualitative appearance, as well as the dentinal tubule diameter. Discriminating however, between the mainland *Elephas antiquus* from the endemic elephants of Tilos island, is more difficult. We measured an important difference in the dentinal tubules' diameter, which is much larger than the dwarf elephant tusks. Additionally, we were able to find a slight variance in the Schreger Pattern, in reference to its qualitative appearance. In particular, the dwarf elephant tusks exhibit the "V" and "C" patterns on

the outer dentine zone ("C" being dominant towards the CDJ), and the inner zone has mostly "X" patterns, while the *E. antiquus* tusks have "V" and "X" motives on the outer part of the Schreger Pattern. We cannot provide a definite explanation for this difference. It may be caused by an alteration in the odontogenetic process. However, changes in the entire appearance of the Schreger Pattern, due to mechanical or chemical alterations, without the simultaneous deformation of the entire tusk, have been mentioned before as a result of the fossilization processes (Agiadi, 2003).

To present, archaeologists have always accepted Asia and Africa as the only source of ivory for the ancient Greeks (Hayward, 1990). However, considering the wealth of Proboscidean tusk findings in many continental and island localities of Greece, fossil ivory should be considered as an alternative source. In particular, tusks of the Pleistocene and Holocene endemic and continental species (i.e. *E. antiquus*, *M. meridionalis* and the dwarf elephants from the Aegean islands) could provide usable ivory. In fact, fossilization would have progressed on these tusks for only a small period of time. Consequently, any alteration of the chemical and structural properties of this ivory may not be severe, by the time the tusks would have to be cut, curved and processed in order to be used. Therefore, the distinction of ivory from different elephant species becomes greatly important in the assessment of such artefacts' true archaeological value. Perhaps some of the archaeological specimens, which are at present thought to be the product of Mediterranean sea trade may, after thorough examination with the above methodology, turn out to have domestic origin. To this end, we propose the review of the ivory specimens found on Greek archaeological sites, examining all the mesoscopic and microscopic features explained in this study, and the comparison of these specimens with paleontologically identified tusks of known origin.

ACKNOWLEDGEMENTS

The Greek General Secretariat for Research and Technology (99 SYN 106 / Project UOA 70/3/4407), the Ministry of Aegean (Project UOA 70/3/699), and the Research Account of the Athens University (Project UOA 70/4/3370) have financed the excavations at the Charkadio Cave. Special thanks are owed to Em.Prof. N. Symeonides who discovered the site and gave us the opportunity to start working there. We would also like to thank Profs. D. Mol and M. R. Palombo for their review of this paper, as well as PhD student E. Stathopoulou for her very helpful remarks on the manuscript.

REFERENCES

- Agiadi, K. 2001. Comparative observations on fossil tusks from three Quaternary Greek localities using scanning electron microscopy. In, *Proceedings of the 1st International Congress "The World of Elephants"*: 523-528. Rome.
- Agiadi, K. 2003. *Introduction to the palaeohistological study of fossil tusks from Greece*. Unpubl. Diplome Paper, University of Athens, Athens. 118 pp.
- Espinoza, E.O. & Mann, M.J. 1993. The History and Significance of the Schreger Pattern in Proboscidean ivory characterization. *Journal of the American Institute for Conservation*, 32: 241-248.
- Fisher, D.C., Trapani, J., Shoshani, J. & Woodford, M.S. 1998. Schreger angles in Mammoth and Mastodon tusk dentin. *Current Research in the Pleistocene*, 15: 105-107.
- Hayward, L.G. 1990. The origin of the raw elephant ivory used in Greece and the Aegean during the Late Bronze Age. *Antiquity*, 64: 103-109.
- Melentis, Joh. 1961. Die Dentition der Pleistozoen Proboscider des Beckens von Megalopolis im Peloponnes (Griechenland). *Annales geologiques des Pays Helleniques*, 12: 153-262.
- Palombo, M.R. 2003. *Elephas? Mammuthus? Loxodonta?* The question of the true ancestor of the smallest dwarfed elephant of Sicily. In Reumer, G.W.F., de Vos, J. & Mol, D. (eds.), *Advances in Mammoth research (Proc. of the 2nd Intern. Mammoth Conference, Rotterdam, May 16-20, 1999)*. *Deinsea*, 9: 273-291.
- Palombo, M.R. & Villa, P. 2001. Schreger lines as support in the Elephantinae identification. In, *Proceeding of the 1st International Congress "The World of Elephants"*: 656-660. Rome.
- Raubenheimer, E.J., Bosman, M.C., Vorster, R. & Noffke, C.E. 1998. Histogenesis of the chequered pattern of ivory of the African elephant (*Loxodonta africana*). *Archives of Oral Biology*, 43: 969-977.
- Schreger, B.N.G. 1800. Beitrag zur geschichte der zaehne. *Beitrage fur die Zergliederungskunst*, 1: 1-7.
- Symeonidis, N.K. & Theodorou, G.E. 1986. On a new occurrence of Lower Pleistocene Proboscidea in South Peloponnese. *Annales geologiques des Pays Helleniques*, 1e serie, 33: 251-261.
- Theodorou, G. 1983. *The dwarf elephants of the Charkadio Cave on the island of Tilos (Dodekanese, Greece)*. PhD dissertation. University of Athens. Athens. 231 pp.
- Theodorou, G. & Agiadi, K. 2001. Observations on the microstructure of fossil tusks from the Charkadio Cave (Tilos, Dodekanese, Greece). In, *Proceeding of the 1st International Congress "The World of Elephants"*: 563-567. Rome.
- Trapani, J. & Fisher, D.C. 2003. Discriminating Proboscidean taxa using features of the Schreger Pattern in tusk dentin. *Journal of Archaeological Science*, 30: 429-438.